



CHORUS

This is the accepted manuscript made available via CHORUS. The article has been published as:

Signatures of pairing in the magnetic excitation spectrum of strongly correlated two-leg ladders

A. Nocera, N. D. Patel, E. Dagotto, and G. Alvarez

Phys. Rev. B **96**, 205120 — Published 13 November 2017

DOI: [10.1103/PhysRevB.96.205120](https://doi.org/10.1103/PhysRevB.96.205120)

Signatures of pairing in the magnetic excitation spectrum of strongly correlated two-leg ladders

A. Nocera,^{1,2} N. D. Patel,^{1,2} E. Dagotto,^{1,2} and G. Alvarez³

¹*Department of Physics and Astronomy, The University of Tennessee, Knoxville, Tennessee 37996, USA*

²*Materials Science and Technology Division, Oak Ridge National Laboratory, Oak Ridge, Tennessee 37831, USA*

³*Computational Science and Engineering Division and Center for Nanophase Materials Sciences, Oak Ridge National Laboratory, Oak Ridge, Tennessee 37831, USA*

Magnetic interactions are widely believed to play a crucial role in the microscopic mechanism leading to high critical temperature superconductivity. It is therefore important to study the signatures of pairing in the magnetic excitation spectrum of simple models known to show unconventional superconducting tendencies. Using the Density Matrix Renormalization Group technique, we calculate the dynamical spin structure factor $S(\mathbf{k}, \omega)$ of a generalized $t - U - J$ Hubbard model away from half-filling in a two-leg ladder geometry. The addition of J enhances pairing tendencies. We analyze quantitatively the signatures of pairing in the magnetic excitation spectra. We found that the superconducting pair-correlation strength, that can be estimated independently from ground state properties, is closely correlated with the integrated low-energy magnetic spectral weight in the vicinity of (π, π) . In this wavevector region, robust spin incommensurate features develop with increasing doping. The branch of the spectrum with rung direction wavevector $k_{rung} = 0$ does not change substantially with doping where pairing dominates, and thus plays a minor role. We discuss the implications of our results for neutron scattering experiments, where the spin excitation dynamics of hole-doped quasi-one dimensional magnetic materials can be measured, and also address implications for recent resonant inelastic X-ray scattering experiments.

PACS numbers:

I. INTRODUCTION

Magnetism is believed to play a key role in the pairing mechanism leading to high critical temperature superconductivity [1–5]. In several materials, the neutron scattering technique is a powerful tool to study magnetic excitations because it can help to identify both their energy and momentum dependence over the entire Brillouin zone. For a wide range of high critical temperature superconductors, including cuprates [6] and pnictides [7–9], an interesting feature of the magnetic excitation spectrum in the superconducting phase is the presence of a resonance peak at a particular wave-vector transfer. In addition, in some cuprates spin incommensurate peaks that develop upon doping have been associated with the presence of stripes [10]. In general, a key challenge in the field of high- T_c superconductivity is to distinguish between universal and nonuniversal properties. In the cuprates, understanding the relationship between the magnetic resonance peak and superconductivity is made difficult by the occurrence of charge stripes and the pseudogap phase. Recent experiments have mapped out the spin excitations in various cuprate families over a large range of energies, [11–15] pointing toward a universal spin excitation spectrum [16] characterized by an “hour-glass” shape with a high-intensity peak at wave vector (π, π) , and both downward and upward dispersing branches of excitations resembling spin incommensurate features.

In early studies of iron-based superconductors a simple picture dominated [7, 8, 17, 18] mostly due to their more itinerant nature. The continuum of magnetic excitations is gapped in the superconducting state, and the

magnetic resonance occurs at an energy below the gap, because of the unconventional symmetry of the superconducting order parameter, and the residual interaction between the quasiparticles that shifts the pole in the total susceptibility to lower energies [17]. Even if in most iron-based superconductors the magnetic resonance has been observed at commensurate wave vectors, recent studies have shown that in doped compounds the resonance could be found at incommensurate wave-vector transfers [19]. However, note that the most recent developments in the field of iron-based superconductors have revisited the weak coupling approximation and Fermi surface nesting rationale [5]. For example there are superconducting compounds that only have electron pockets at the Fermi level [20]. In fact, evidence is accumulating that pnictides and chalcogenides are in the difficult intermediate coupling regime where neither a fully itinerant nor a fully localized picture is valid.

To better guide experiments, it is therefore of considerable importance to investigate theoretically the magnetic excitations spectra of model Hamiltonians that present unconventional superconducting tendencies in their ground states. However, this task is technically formidable. In layered geometries, there are no reliable computational techniques to address the ground state properties of the system doped away from half-filling at the low temperatures characteristic of superconductivity. For example, Quantum Monte Carlo techniques suffer from sign problems. In addition, the study of dynamical magnetic spectral functions, such as $S(\mathbf{k}, \omega)$, are also challenging due to the limitations of Maximum Entropy procedures.

For all these reasons, it is imperative to find a simple example where computational techniques allow for the simultaneous and accurate calculation of both ground state pairing properties as well as dynamical spectral functions. In this publication, we provide the first steps in this direction by carefully analyzing the Hubbard model defined on a two-leg ladder, supplemented by a superexchange J to boost further the pairing tendencies, using the Density Matrix Renormalization Group (DMRG) technique [21], both addressing the ground state as well as its dynamical properties. Our main challenge is: can we identify features in the dynamical spin-structure-factor that appear proportional to the pairing strength? In this work, we will show that *in the case of two-leg ladders ground state pairing properties are correlated with the low-energy spin excitations spectral weight of the system close to the magnetic wave-vector transfer (π, π)* .

In the 90's, model Hamiltonian studies of copper-oxide two-leg ladders were fruitful in elucidating several physical properties of their two dimensional counterparts [22, 23]. Experimentally, the intrinsically doped $\text{Sr}_2\text{Ca}_{12}\text{Cu}_{24}\text{O}_{41+\delta}$ two-leg ladder material was found to become superconducting under pressure [24], establishing a strong link between two-leg ladders and layer-based cuprates. Indeed, in striking similarity with the underdoped two-dimensional cuprates, the doped $t - J$ and Hubbard ladders show superconducting tendencies, as described in [22, 23, 25–29]. Recently, the authors of [30] have revisited the crucial question of which is the dominating instability in doped Hubbard ladders employing state-of-the-art computational procedures, concluding in favor of pairing in the limit of small doping.

The study of the dynamical magnetic properties of superconducting ladders have received less attention. In [31], the dynamical spin structure factor of doped two-leg $t - J$ ladders were studied, concluding that a hole pair-magnon bound-state evolves into a magnetic resonant excitation at finite hole doping. That study was performed with Lanczos exact diagonalization on $L = 12 \times 2$ clusters. Ring exchange terms were proven to be important to understand the spin dynamics of insulating cuprate materials [32–34]. With this motivation, in [35] the dynamical spin spectrum of doped $t - J$ ladders with ring exchange interactions were studied as well. Recently, an analytical low-energy effective field theory description of the doped Hubbard two-leg ladder model also reported [36] an incommensurate coherent mode near (π, π) .

The present work aims to fill the gaps in the above mentioned literature by investigating in detail the dynamical spin spectrum of a generalized $t - U - J$ model using the DMRG method. In this regard, it was argued that in a pure Hubbard model the exchange correlation strength is constrained by the local Hubbard repulsion to be proportional to $J \sim t^2/U$, and pairing tendencies are difficult to observe due to the competition with other phases (CDW or stripe-like phases). If the pairing correlation strength is linked to the effective exchange interaction strength, this would tend to zero in the limit of

infinite Hubbard repulsion. For this reason, it was proposed [37–40] that a more realistic model of the cuprates is given by a generalized $t - U - J$ model, because this model allows for an exchange magnetic interaction J that is independent of U .

In a two-leg ladder geometry—the main focus of this paper—previous efforts found [37] that pairing tendencies are enhanced as “extra” superexchange interactions J are added to the Hubbard model. While the pairing tendencies in the ground state after introducing J have been studied [37, 41, 42], the computation of the magnetic excitation spectrum of the $t - U - J$ model has not been reported until now.

The main aim of this paper is the following. We wish to analyze whether the magnetic spectrum of two-leg ladders displays features that are correlated with the pairing tendencies known to be present in the ground state. In other words, we wish to establish a correspondence between pairing properties, directly measured in the ground state, with properties of the magnetic spectrum that can be measured via neutron scattering experiments. Our main conclusion is that varying hole doping, the low-energy integral of the magnetic spectral weight in the vicinity of (π, π) correlates qualitatively with the pairing correlation strength deduced from pair-pair correlations in the ground state. We also observed that the portion of the magnetic spectrum related with wavevector 0 along the rung direction, as opposed to π , does not seem related to pairing.

Our results have implications not only for neutron scattering but also for resonant inelastic X-ray scattering (RIXS) experiments. Indeed, RIXS has recently emerged as a complementary tool to neutron scattering to study the magnetic excitations of strongly correlated materials [43]. In particular, recent RIXS investigations of $\text{La}_{2-x}\text{Sr}_x\text{CuO}_4$ (LSCO) have reported the persistence of high energy magnetic excitations from the underdoped up to the highly overdoped regime where superconductivity disappears [44–46], raising questions about the role of these excitations in the pairing mechanism for cuprates. In contrast, neutron scattering experiments have shown that low energy magnetic excitations around the antiferromagnetic zone center “disappear” with sufficient hole doping [47]. These contrasting results have been reconciled theoretically in [48], confirming the persistence of high energy magnetic excitations along the antiferromagnetic zone boundary while pointing to the important role of magnetic excitations around the antiferromagnetic zone center (π, π) in the pairing mechanism. Recently, another theoretical investigation [49] of the two-dimensional Hubbard model employing Quantum Monte Carlo and Maximum Entropy techniques varying doping has confirmed that high energy magnetic excitations are marginal to the pairing mechanism, while the main reason for the reduction of the pairing strength (and of the superconducting transition temperature T_c) is related with the redistribution of spectral weight at wave-vector momentum transfers not accessible to RIXS experiments.

In [50], RIXS and neutron scattering measurements of the same LSCO sample demonstrated that the two techniques can probe magnetic excitations in complementary regions of the Brillouin zone, showing that the contrast between the results obtained with the two approaches could be solved also experimentally in the future.

This work is organized as follows. Section II introduces the $t-U-J$ model, and briefly reviews its known limiting cases: the Hubbard and $t-J$ models. Section III contains the main results. In sections III.A and III.B we present the ground state properties and the magnetic excitation spectrum of a $t-U-J$ ladder at fixed realistic hole doping and Hubbard repulsion, changing the magnetic exchange interaction J . Section III.C explores the properties of the magnetic excitations at the same doping but now as a function of local Hubbard repulsion U , at $J = 0.0$. Section III.D reports the analysis of the dependence of the magnetic excitation spectrum as a function of the hole doping, and its correlation with ground state pairing properties. In Section IV we provide our conclusions.

II. GENERALIZED HUBBARD MODEL

The Hamiltonian of the generalized $t-U-J$ model defined on a two-leg ladder geometry is

$$\begin{aligned}
H = & \left(-t_x \sum_{\substack{\langle i,j \rangle \\ \sigma, \gamma=0,1}} c_{i,\gamma,\sigma}^\dagger c_{j,\gamma,\sigma} - t_y \sum_{i,\sigma} c_{i,0,\sigma}^\dagger c_{i,1,\sigma} \right) + \text{h.c.} \\
& + U \sum_{i,\gamma=0,1} n_{i,\gamma,\uparrow} n_{i,\gamma,\downarrow} + J_x \sum_{i,\gamma=0,1} \left(\vec{S}_{i,\gamma} \cdot \vec{S}_{i+1,\gamma} + \right. \\
& \left. - \frac{1}{4} n_{i,\gamma} n_{i+1,\gamma} \right) + J_y \left(\sum_{i,\sigma} \vec{S}_{i,0} \cdot \vec{S}_{i,1} - \frac{1}{4} n_{i,0} n_{i,1} \right), \quad (1)
\end{aligned}$$

where $c_{i,\gamma,\sigma}^\dagger$ ($c_{i,\gamma,\sigma}$) creates (destroys) an electron at leg $\gamma = 0, 1$ on site $i = 0, \dots, L/2-1$ and spin $\sigma = \uparrow, \downarrow$, where L represents the total number of sites, $L/2$ for each leg. In this work, a ladder with open boundary conditions along the leg direction is considered. In the Hamiltonian above, the term $-\frac{1}{4} n_{i,\gamma} n_{i+1,\gamma}$ has been included because it is present in the standard definition of the t - J model [51]. $n_{i,\gamma}$ and $\vec{S}_{i,\gamma}$ represent the electronic occupation operator (summed over spins) and spin operators on site i and leg γ . Following standard notation, t_x and t_y represent the hopping parameters in the x (along the leg) and y (along the rung) direction of the ladder. For simplicity, in most figures the y direction wavevector will be explicitly indicated as k_{rung} while the x direction wavevector will be denoted as k . J_x and J_y are the exchange interactions along the leg and rung directions, respectively. U is the local Hubbard on-site Coulomb repulsion strength. We consider $t_x = t_y = 1$ as unit of energy, and $J_x = J_y = J$ for the exchange interaction. The model above reduces to the standard Hubbard model for $J = 0$, and to the standard $t-J$ model for $U \rightarrow \infty$, as double electronic occupation is forbidden in this limit.

Let us recall the basic properties of the standard Hubbard ladder, recovered from Eq. (1) in the $J = 0$ limit. In the symmetric $t_x = t_y$ and non-interacting $U = 0$ case, both bonding (+) and antibonding bands (-), $\epsilon_\pm = -2(\cos(k_x) \mp 1)$, are partially filled by electrons if the electronic density $n = N_{el}/L$ is larger than quarter-filling, $n = 0.5$, where N_{el} is the total number of electrons. Only the case of $n \geq 0.50$ will be considered in this paper. When $n \geq 0.50$, there are then four Fermi points: $\pm k_{F+}$ for the bonding and $\pm k_{F-}$ for the antibonding bands. At generic filling n , $k_{F+} + k_{F-} = \pi n$. At half-filling and $U > 0$ the Hubbard ladder has both a charge and spin gap. Away from half-filling, the charge gap disappears, while the spin gap decreases remaining finite up to large finite doping [52–55]. Moreover, the system presents power law $d_{x^2-y^2}$ -like pair-field correlations [30, 56].

The $t-J$ model on ladders has been thoroughly studied in the cuprates literature [22, 23, 25]. In the undoped limit, it has been well established that the $t-J$ model has a spin gap due to the particular ladder geometry which favors the spin singlet formation along rungs, and the physics can be well described in terms of the Heisenberg ladder model. Upon doping, superconducting tendencies develop [22, 25–29]. The physics of $t-J$ (and Hubbard) two-leg ladders has been studied with many techniques ranging from Exact Diagonalization to DMRG to bosonization [57]. Away from half-filling, the spin gap and superconducting binding energy of hole pairs was studied in [58] showing that they can be maximized by tuning the anisotropic ratios to $t_y/t_x \simeq 1.25$ and $J_y/J_x \simeq 1.56$. In general, and important for the goals of our present publication, in [59] it was explained that neutron scattering data could provide important evidence for the pairing mechanism based on the exchange interaction J . For this reason we aim to study in parallel the pairing ground state properties of ladders introducing doping, as well as the inelastic neutron scattering spectrum $S(\mathbf{k}, \omega)$ under similar circumstances and analyze whether correlations among them can be established.

The DMRG correction-vector method has been used throughout this paper [60]. Within the correction vector approach, we use the Krylov decomposition [61] instead of the conjugate gradient. An application of the method to Heisenberg and Hubbard ladders at half-filling can be found in [62]. In this work, a $L = 48 \times 2$ ladder has been simulated, using $m = 1000$ DMRG states with a truncation error kept below 10^{-5} . The spectral broadening in the correction-vector approach has been considered fixed at $\eta = 0.08t$. The DMRG implementation used throughout this paper has been discussed in detail in [62]; technical details are in the Supplemental Material [63].

III. RESULTS

A. Enhancement of pairing tendencies by J

We begin by studying the ground state properties of a $L = 48 \times 2$ ladder at a fixed doping $n = 0.875 = 84/96$. This filling was chosen because it has been widely used to study pairing tendencies on ladders, such as in [37], and because the spectrum features to be described below are sharp and clearly visible. Thus $n = 0.875$ is an ideal doping for a preliminary understanding of the dynamical structure factor.

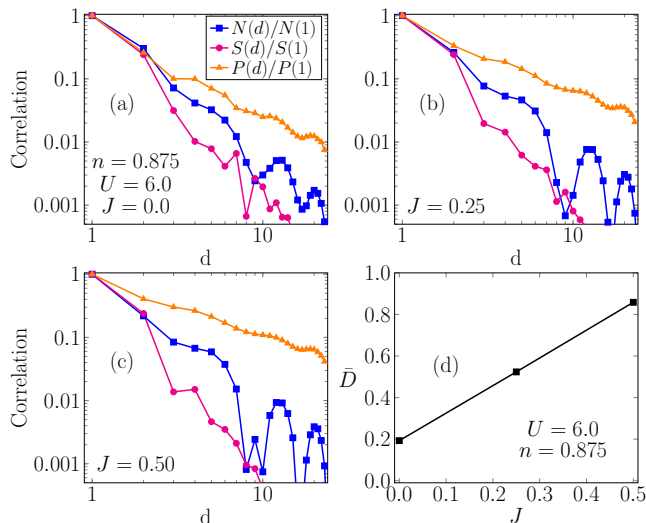


FIG. 1: (Color online) Panels (a-b-c): Charge, spin, and rung-singlet pair correlation functions versus distance along the ladder leg for different values of the magnetic exchange interaction J . Note that in these panels the results are normalized to those at distance 1. Panels (d): Pairing correlation strength (see text) as a function of magnetic exchange interaction J . A $L = 48 \times 2$ ladder has been simulated, with electronic filling $n = 0.875 = 84/96$. The number of DMRG states kept is $m = 1000$.

We have checked that our results are in agreement with an early study of the same model [37] for a shorter system size, $L = 32 \times 2$. Figure 1(a-b-c) shows the *averaged* rung-singlet pair correlation function $P(d)$, rung spin $S(d)$, and rung density correlation $N(d)$ calculated as a function of the distance d along the leg of the ladder for different values of the magnetic exchange interaction J , fixing the Hubbard repulsion to an intermediate value $U = 6.0$. The *averaged* correlation function for a generic operator \hat{O} is defined as

$$O(d) = \frac{1}{L-d} \sum_{j=1}^{L-d} \langle \hat{O}_j^\dagger \hat{O}_{j+d} \rangle. \quad (2)$$

We have a rung-singlet pair correlation $P(d)$ when

$\hat{O} = \Delta_i$, with the operator Δ_i^\dagger defined as

$$\Delta_i^\dagger = \frac{1}{\sqrt{2}} \left(c_{i,0,\uparrow}^\dagger c_{i,1,\downarrow}^\dagger - c_{i,0,\downarrow}^\dagger c_{i,1,\uparrow}^\dagger \right). \quad (3)$$

For the rung spin correlations we have used $\hat{O}_i = \sum_{\gamma=0,1} \hat{S}_{i,\gamma}$, while for the rung density correlation $N(d)$ we employed $\hat{O}_i = \sum_{\gamma=0,1} n_{i,\gamma}$.

Our results in Fig. 1(a-b-c) confirm that the “extra” exchange interaction J increases the strength of the pairing, and induces a slower decay of the rung-singlet pair correlation function as compared with the case $J = 0$. Moreover, Figure 1 shows also that the rung density and rung spin correlation functions have a faster decay than the pair correlations. We can therefore conclude that the increase of the magnetic exchange interaction J *increases pairing to a point where it dominates*. This is also shown in Fig. 1(d) where the pairing correlation strength is estimated by evaluating the quantity $\bar{D} = \sum_{i=6}^{12} P(i)/P(1)$ (note that 6 and 12 are *arbitrary* lower and upper bounds in the sum, see supplemental material [63]). In fact \bar{D} increases approximately linearly as a function of J . Our results are also in agreement with [30], where a careful size scaling analysis of the correlation function was performed on a doped Hubbard ladder, concluding that superconducting correlations are dominant in the regime that we also investigate in this work.

B. Magnetic excitations at fixed hole doping changing J

At each frequency ω , we compute the dynamical spin structure factor of the two-leg ladder in real space

$$S_{j,c}(\omega + i\eta) = \langle \Psi_0 | S_j^z \frac{1}{\omega - H + E_g + i\eta} S_c^z | \Psi_0 \rangle \quad (4)$$

for all sites of the lattice, where E_g is the energy of the ground state $|\Psi_0\rangle$ of the Hamiltonian H . Above, $j \equiv (j_x, j_{rung})$ corresponds to the two coordinates of the site on the ladder, where $j_{rung} = 0$ ($j_{rung} = 1$) for the lower (upper) leg of the ladder. The center site is $c \equiv (L/4 - 1, 0)$. The above quantity is then Fourier transformed to momentum space giving two components

$$\begin{aligned} S((k_x, k_{rung} = 0), \omega) &= \sqrt{\frac{2}{L/2+1}} \sum_{j_x=0}^{L/2-1} \sin((j_x+1)k_x) \times \\ &\quad \times [S_{(j_x,0),c}(\omega + i\eta) + S_{(j_x,1),c}(\omega + i\eta)], \\ S((k_x, k_{rung} = \pi), \omega) &= \sqrt{\frac{2}{L/2+1}} \sum_{j_x=0}^{L/2-1} \sin((j_x+1)k_x) \times \\ &\quad \times [S_{(j_x,0),c}(\omega + i\eta) - S_{(j_x,1),c}(\omega + i\eta)], \end{aligned} \quad (5)$$

where the quasi-momenta $k_x = \frac{\pi n}{L/2+1}$ with $n = 1, \dots, L/2$ are appropriate for open boundary conditions on each

leg. To simplify the notation, we will consider $k_x \equiv k$ below.

Figure 2 shows the dynamical spin structure factor of the ladder changing the value of the exchange interaction J for the same parameters investigated above.

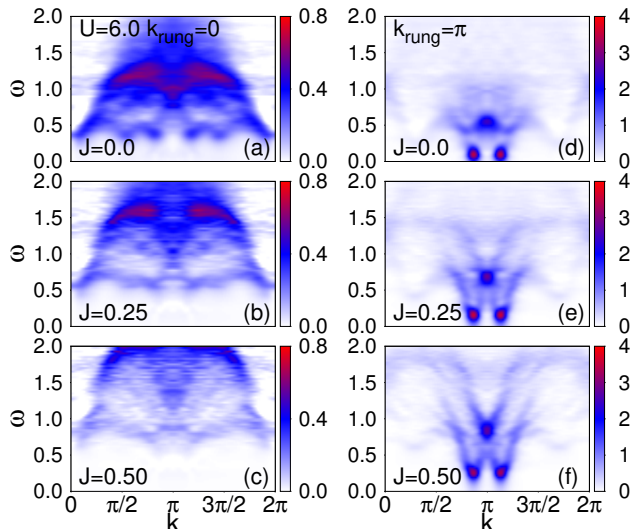


FIG. 2: (Color online) Panels (a-b-c): $k_{rung} = 0$ component of the magnetic excitation spectrum for a $t - J - U$ ladder using $L = 48 \times 2$ sites and the DMRG technique at $U = 6$ and filling $n = 0.875 = 84/96$. Panel (a) corresponds to $J = 0.0$, (b) to $J = 0.25$, and (c) to $J = 0.50$. Panels (d-e-f): $k_{rung} = \pi$ component of the magnetic spectrum for the same parameters used above. The number of DMRG states kept is $m = 1000$.

Figures 2(a) and (d) show the magnetic excitation spectrum for a doped Hubbard ladder at $J = 0.0$. In the $k_{rung} = 0$ component (a), an umbrella-like shape manifold of excitations appears above a robust gap, for the value of doping chosen. As the exchange magnetic interaction J increases, one can observe that the region of depleted weight at $k_{rung} = 0$ also increases and the entire spectrum is pushed up in energy, but the shape of the dispersion of the low-energy excitation band does not change qualitatively with J . However, the amplitude of the low energy sinusoidal oscillations in the magnetic dispersion are damped by the extra magnetic exchange interactions.

In the $k_{rung} = \pi$ component of the magnetic spectrum Fig. 2(d), most of the spectral weight is concentrated at the incommensurate wave-vector $k_x \simeq \pi n$ (with the companion peak at $2\pi - \pi n$; x is the leg direction) as it can also be observed in the static structure factor (not shown). These sharp peaks do not seem to be separated in energy from the rest of the spectrum at higher energy, at least within the resolution of our study. Indeed, our data does not contain features that could be associated with a bound state magnetic excitation distinctly separated below a continuum of excitations at this hole-doping density, and we have also verified this observation

for a shorter system size, $L = 32 \times 2$. Namely, we cannot distinguish a clear “resonance” feature in the spin excitations even though ground state measurements indicate that pairing tendencies are dominant. However, although the subtle issue of the existence of a resonance merits further elaboration, our focus in the rest of the manuscript is quite different, as explained below. Figure 2(d) suggests that at $J = 0.0$ from each sharp low-energy peak a linear branch of higher energy excitations with smaller spectral weight develops, with reflection symmetry with respect to $k_x = \pi$. Another visible broad band of excitations occurs at high energy around $\omega/t \simeq 0.5$, with a central peak around $k_x = \pi$.

These $k_{rung} = \pi$ spectral features described above are enhanced and clarified when “extra” exchange interactions are introduced compared to the pure Hubbard model obtained for $J = 0.0$. With increasing J the spin gap of the incommensurate spin excitations increases, while their intensity remains approximately the same with increasing J . This is interesting because J increases the pairing tendencies in the ground state. Moreover, we observe that by increasing J , spectral weight leaks to the triangle-shape area between the incommensurate peaks and the higher energy peak at (π, π) which occurs around $\omega \simeq 0.9$ for $J = 0.5$. As we will explain in section III.D, we will use the low energy spectral weight around (π, π) as a measure of the pairing correlation strength in the system and we will find that it increases with J . As the exchange magnetic interactions are increased, the W -shaped energy spectral feature observed in the $k_{rung} = \pi$ component of the magnetic excitation spectrum at $\omega/t \simeq 0.5$ for $J = 0.0$ is pushed to higher energies, with two long V -shape spectral bands developing, starting from the incommensurate low energy peaks. These two spectral features intersect at (π, π) at higher energy transfer which increases with J . We can summarize the results of this section by stating that the “extra” exchange interaction J mainly shifts the magnetic spectrum to higher energies, maintaining the dispersive features of the magnetic excitations qualitatively unchanged.

C. Magnetic excitations at fixed hole doping changing U

In this section, we study the magnetic excitation spectrum of the doped ladder ($n = 0.875$) at $J = 0.0$ for different values of the on-site Hubbard repulsion U . By studying the ground state rung-singlet pair correlations, we have found that the pairing correlation strength increases with U starting from $U = 0.0$, it reaches a broad maximum in the range $U \sim 4 - 6$, and eventually decreases as U is further increased. Analogously, we have found that also the spin gap has a similar behavior, reaching a maximum for $U \sim 4 - 6$ as in the case of half-filling [37, 62]. These results agree with those reported in [37], supporting the notion that Hubbard on-site re-

pulsion reduces charge and spin fluctuations such that pairing dominates at intermediate U , while for very large U spin fluctuations will eventually dominate over pairing.

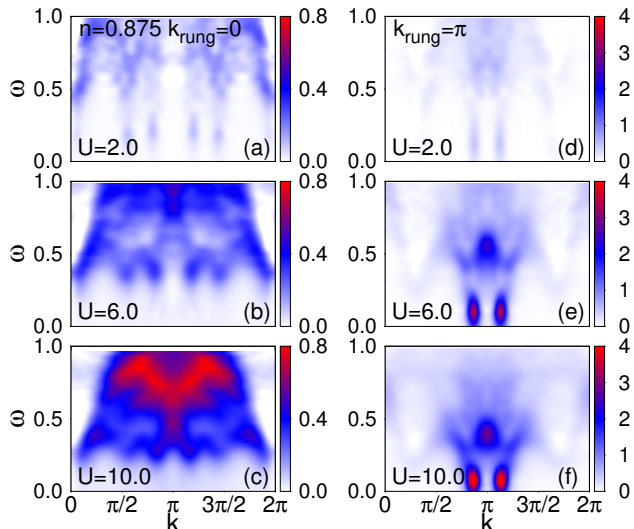


FIG. 3: (Color online) Panels (a-b-c): $k_{rung} = 0$ component of the magnetic excitation spectrum obtained with DMRG for a t - J - U ladder of $L = 48 \times 2$ sites, at $J = 0.0$ and $n = 0.875$. Panel (a) corresponds to $U = 2.0$, (b) to $U = 6.0$, and (c) to $U = 10.0$. Panels (d-e-f) are the $k_{rung} = \pi$ component of the magnetic spectrum, for the same parameters as above.

Figure 3 shows the dynamical spin structure factor of our doped ladder changing the value of U at $J = 0.0$. Panels (a,b,c) of Fig. 3 display the $k_{rung} = 0$ component of the magnetic excitation spectrum. At $U = 2.0$ the results are still similar to the noninteracting limit. At $U = 6.0$ and beyond, there is a gap at low energy that closes with increasing U , keeping approximately the overall shape of the spectrum. There are no dominant coherent peaks. The sinusoidal oscillations of the lower energy magnetic excitations are damped as U increases. Overall, similarly as in the previous analysis varying J , the $k_{rung} = 0$ portion of the spectrum contains broad features but not much coherence.

Figures 3(d-e-f) show the $k_{rung} = \pi$ component of the magnetic excitation spectrum for the same parameter values investigated above. A spectral redistribution from high energy to low energy is observed, as in the $k_{rung} = 0$ component of the spectrum. In [62], where the crossover Hubbard-to-Heisenberg behavior in the half-filled case was carefully studied, a similar spectral weight redistribution was observed. At $U = 2.0$ the results resemble the non-interacting case with very low weight in the energy range studied. As U increases, sharp incommensurate peaks develop at low energies (note the change in the intensity convention between left and right panels), similarly as when J was varied before at fixed $U = 6.0$.

We can summarize the results of this subsection by stating that increasing from zero the on-site Hubbard repulsion, the spectral weight much increases at

intermediate-low energies in both branches. The $k_{rung} = 0$ component remains disorganized varying U , but the $k_{rung} = \pi$ component develops coherent sharp peaks at low energies that likely dominate the physics related with the interaction between the charge and spin degrees of freedom.

D. Magnetic excitations as a function of hole doping

This section investigates the properties of the magnetic excitation spectrum for our $t - U - J$ ladder now as a function of hole doping, at a fixed value of the Hubbard interaction $U = 6.0$, and attempts to correlate some of its features with the pairing strength in the ground state.

1. Pairing correlation strength varying n

Figure 4(a) shows the ground state rung-singlet pair correlations versus distance, along the ladder leg, at the different values of the electronic filling indicated. Note that the results are normalized to distance 1. At half-filling the pair correlations decay to zero exponentially fast, giving a very small pairing correlation strength. At $J = 0.0$, namely without any extra J boost for hole binding, the results indicate that the pairing correlation strength (panel (b)) increases rapidly with hole doping starting from the half-filled case, develops a broad maximum, and then decreases reaching almost zero at $n = 0.5$. The actual values of the pairing correlation strength are sensitive to the choices of lower and upper limits in the definition of \bar{D} but the overall shape is qualitatively stable (see also the supplemental material [63]), displaying an asymmetric superconducting dome, that remains approximately the same as the magnetic exchange interaction increases. Note that in the range from $n = 0.75$ to $n = 0.5833$ the pairing strength is nearly constant, which is somewhat surprising: intuitively a monotonous decrease of \bar{D} from the peak near half-filling towards the near zero value at quarter-filling would have been more natural. This anomalous behavior will be addressed in future investigations. However, our focus in the rest of the publication will be on the more robust and stable feature related with the clear dominant peak near half-filling and its correlation with magnetism.

2. Magnetic spectrum varying n

To study whether there are signatures of the pairing tendencies unveiled above in the magnetic excitation spectrum, Fig. 5 and Fig. 6 show the $k_{rung} = 0$ and $k_{rung} = \pi$ components of the dynamical spin structure factor at $J = 0.0$, respectively, for similar values of electron fillings as investigated above for pairing.

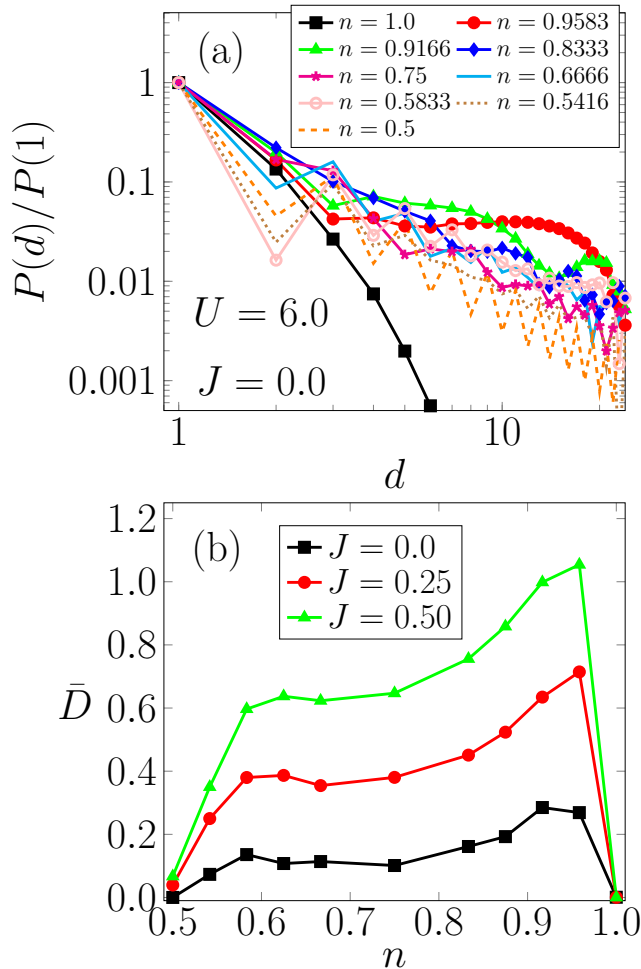


FIG. 4: (Color online) (a) Pair correlation functions corresponding to rung-singlet pairs versus distance, at several values of the electronic filling n (see inset), and at a fixed $U = 6.0$ and $J = 0.0$. The data is normalized to distance one. These correlations are very weak at $n = 1$, rapidly develop with reducing n , and then drop again at $n = 0.5$. (b) Pairing correlation strength (defined as $\bar{D} = \sum_{i=6}^{12} P(i)$, see text) versus electron filling n , at $U = 6.0$ and the values of J indicated in the inset.

Figure 5 shows that by decreasing the electronic filling, the $k_{\text{rung}} = 0$ component of the magnetic excitation spectrum maintains qualitatively its structure in the interval of fillings $0.8333 \leq n < 1$. Our results are consistent with recent studies of the magnetic spectrum of the two-dimensional Hubbard model varying doping [49], where it was observed that the dispersion of the magnetic excitations along the line $(0,0) - (\pi,0)$ in the Brillouin zone does not change much with hole doping, while at the same time the pairing correlation strength was found to be reduced. Similarly, our results also indicate that the $k_{\text{rung}} = 0$ branch of the ladder spectrum does not seem correlated with pairing either.

At $n = 0.75$ and lower densities, a low-intensity low-energy feature at the leg wavevector $k = \pi$ develops.

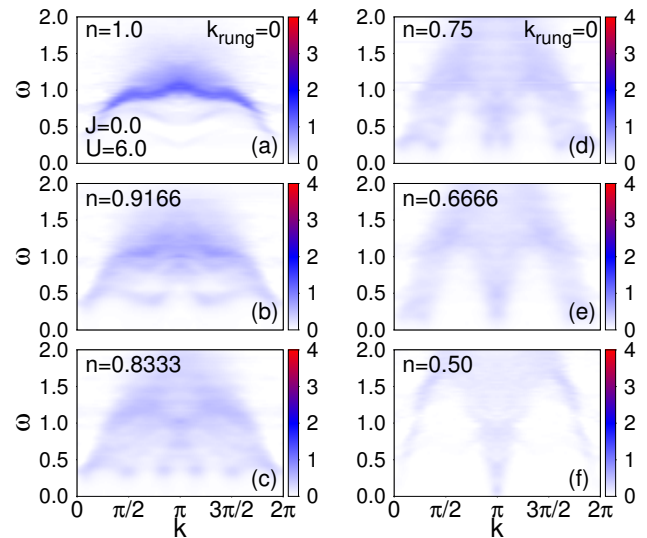


FIG. 5: (Color online) $k_{\text{rung}} = 0$ component of the magnetic excitation spectrum for a $t - J - U$ ladder using $L = 48 \times 2$ sites and the DMRG technique, at $U = 6.0$ and $J = 0.0$, and at the several electronic fillings n indicated.

This feature resembles results found already in the non-interacting limit $U = 0.0$ at these densities indicating that this portion of the magnetic spectrum represents quasi non-interacting electrons.

Figure 6 shows that the $k_{\text{rung}} = \pi$ component contains much more of the total spectral weight of the magnetic excitations. In particular, we can observe at half-filling (panel (a)) the typical V-shape-like of the magnetic excitation dispersion which is characteristic of the Heisenberg counterpart [62] where the spectral weight is mainly concentrated at the scattering wave-vector (π, π) . In this case, the Fermi momentum $k_F = \pi n$ is equal to π at half-filling ($U = 6.0$ is strong and it is mainly accidental that such a weak coupling based on the Fermi momentum perspective is still valid).

Upon decreasing the electronic filling, the magnetic excitation peak at (π, π) splits in two incommensurate peaks as observed also in the previous sections at $n = 0.875$, with separation in momentum transfer proportional to the electronic filling itself, $2k_F = 2\pi n$. At the same time, it is evident that the spectral weight redistributes at smaller momentum transfers, so that overall the scattering region in the interval $(\pi/2, 3\pi/2)$ around (π, π) becomes depleted in spectral weight by hole doping. Although it can be barely noticed in the scale used, we found that the spin gap that characterizes ladders at half-filling is monotonically reduced with hole doping (the wavevector position that characterizes the spin gap is that of the incommensurate features, when at finite doping). The fine details of how this occurs are not important because it will be discussed below that the *integral* of the spectral weight near (π, π) is what correlates with the ground state pairing properties. Finally, at $n = 0.5$ we observe that the spectral weight is mostly con-

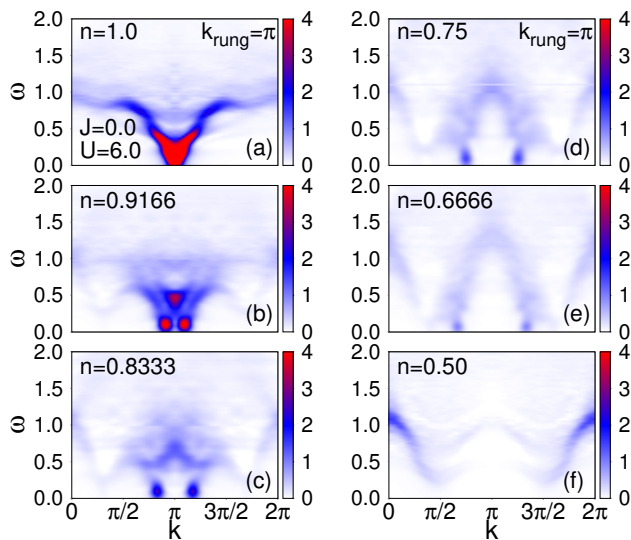


FIG. 6: (Color online) $k_{rung} = \pi$ component of the magnetic excitation spectrum for a $t - J - U$ ladder using $L = 48 \times 2$ sites and the DMRG technique, at $U = 6.0$ and $J = 0.0$, and at the several electronic fillings n indicated.

centrated at $(0, \pi)$, with highly dispersive spectral bands appearing in the intervals $(0, \pi/2)$ and $(3\pi/2, 2\pi)$.

Considering that J increases the tendencies to superconduct, it is also interesting to analyze the magnetic spectral properties at, e.g., $J = 0.25$. The results are in Figs. 7 and 8. For the $k_{rung} = 0$ branch, the shape of the dominant features is approximately the same as for $J = 0.0$. As expected from previous analysis, overall there is a shift to higher energies of the spectrum. Similar conclusions were reached for the $k_{rung} = \pi$ branch: clearly the dominant features qualitatively are the same varying J . However, overall the intensity of the low energy excitations increases with increasing J . Thus, *the low-energy intensity near (π, π) is the property that appears the closest related to pairing*.

We can partially summarize these results by stating that the magnetic excitations dispersion along the line $(0, 0) - (\pi, 0)$ in the Brillouin zone do not change substantially against hole doping. On the other hand, the pairing correlation strength rapidly increases starting from half-filling $n = 1.0$, reaching a maximum around $n \simeq 0.9$ and then further decreasing by hole doping. At the same time, a significant spectral weight redistribution away from the (π, π) wavevector, characteristic of the half-filled case, is observed as a function of hole-doping, with the overall intensity decreasing with doping. It seems that pairing and the overall weight near (π, π) are correlated.

To better characterize quantitatively this spectral weight redistribution, we have evaluated the integrated low-energy spin spectral weight around the wave-vector transfer (π, π) as a function of hole doping (see Fig. 9). In particular, we have integrated the dynamical spin structure factor in the following rectangular region $k_x \in [k_F, \pi]$, $\omega \in [0, \Delta_S]$, where Δ_S is the spin gap at half-

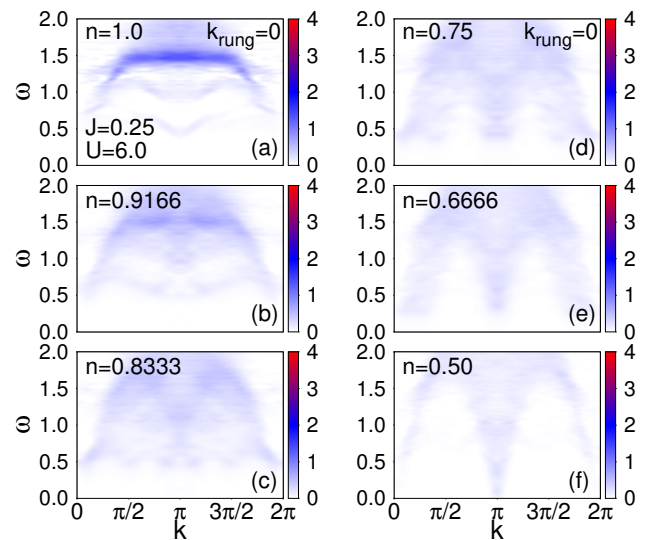


FIG. 7: (Color online) $k_{rung} = 0$ component of the magnetic excitation spectrum for a $t - J - U$ ladder using $L = 48 \times 2$ sites and the DMRG technique, at $U = 6.0$ and $J = 0.25$, and at the several electronic fillings n indicated.

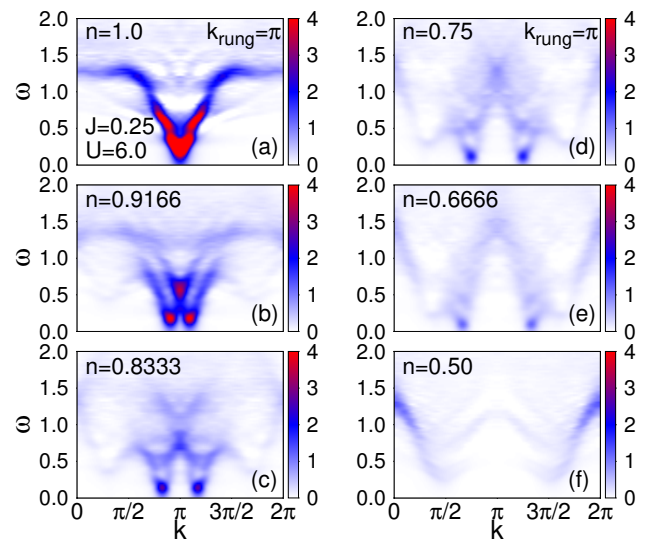


FIG. 8: (Color online) $k_{rung} = \pi$ component of the magnetic excitation spectrum for a $t - J - U$ ladder using $L = 48 \times 2$ sites and the DMRG technique, at $U = 6.0$ and $J = 0.25$, and at the several electronic fillings n indicated.

filling (in practice Δ_S is 0.125, 0.25 and 0.375, at $J = 0.0$, 0.25, and 0.50, respectively), defining:

$$\bar{D}_S = \int_{k_F=\pi n}^{\pi} dk_x \int_0^{\Delta_S} d\omega S(k_x, \pi, \omega). \quad (6)$$

By construction, the quantity above is zero at half-filling, because there is no weight below the spin gap plus in this case k_F reaches π . This corresponds to the intuitive notion that, even if the binding energy for hole-pairs is finite in the half-filled case indicating hole pair tenden-

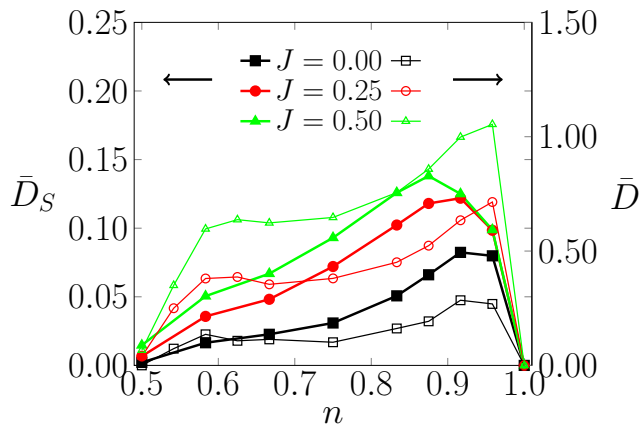


FIG. 9: (Color online) Low energy spin spectral weight \bar{D}_S (left y-axis) defined in Eq. 6 and pairing correlation strength \bar{D} (right y-axis) computed from ground state as a function of electron filling for the values of J indicated.

cies, if there are no holes in the system then there are no carriers that can generate robust pair-pair correlation functions. Only if there is a finite concentration of holes, the magnetic mechanism can bind holes leading to a superconducting phase. Thus, the quantity defined above is qualitatively consistent with expectations for pairing in a doped magnetic system. Based on results for 600, 800, and 1000 DMRG states, we have verified that the relative error on the \bar{D}_S values extracted from the $S(k, \omega)$ are approximately 5% in this range of DMRG states used.

By hole doping, spin spectral weight is progressively transferred to the domain region of integration (which increases as n decreases from 1) as a consequence of the commensurate-to-incommensurate effect observed, e.g., moving from $n = 1$ to $n = 0.9166$ in panels (a-b) of Fig. 6. The results in Fig. 9 show that the low-energy spin spectral weight reaches a maximum at $n \simeq 0.925$ for $J = 0.0$, while the dominant peak slightly shifts to lower values as one increases the magnetic exchange interactions: \bar{D}_S peaks at $n \simeq 0.9$ for $J = 0.25$ and at $n \simeq 0.875$ for $J = 0.50$. For larger hole dopings, \bar{D}_S decreases reaching its minimum for $n = 0.5$.

Results in Fig. 9 clearly display similarities with the pairing strength studied in Fig. 4(b) suggesting that the quantity \bar{D}_S can be qualitatively used as a measure of the pairing strength and it can be extracted experimentally from the magnetic excitation spectra. Even the anomalous pairing-related “bump” at $n = 0.5833$ in Fig. 4(b) also appears as a mild feature in Fig. 9. These similarities should not be underestimated: Fig. 9 was obtained totally from magnetism, and independently of any pairing measurement in the ground state.

IV. SUMMARY AND CONCLUSIONS

In this publication, we have studied the pairing properties and magnetic excitation spectra of a generalized

Hubbard model ($t - U - J$ model) on a ladder geometry. We have analyzed the behavior of the system by changing the magnetic exchange interaction J , the on-site Hubbard repulsion U , and the electronic filling n .

With regards to ground state properties, our analysis confirms that the dominance of pairing correlations increases as the strength of the superexchange interaction J increases. For the case of $J = 0.0$, pairing is optimized for a Hubbard repulsion $U = 6.0$ at the widely used electronic filling $n = 0.875$. Moreover, the pairing correlations strength has an “asymmetric superconducting dome” shape with a broad maximum around 5–10% hole doping, remaining robust over a wide range of hole densities until it becomes negligible at 50% doping.

We have focused on providing a detailed analysis of the magnetic excitation spectrum and we searched for connections with the pairing properties of the doped ground state. With regards to the addition of the “extra” exchange interaction J , this new term mainly shifts the magnetic spectrum to higher energies, but qualitatively keeps unchanged the shape of the dispersive features. Interestingly, we noticed that by increasing J spectral weight increases in the low energy region around (π, π) . Analogously, by increasing the on-site Hubbard repulsion, the spectral weight redistributes from high to intermediate-low energies, maintaining approximately the shape of the main features.

More importantly, we have studied the properties of the dynamical spin structure factor as a function of hole doping. The results indicate that the magnetic excitations dispersion along the line $(0, 0) - (\pi, 0)$ in the Brillouin zone, namely in the $k_{rung} = 0$ branch of the spectrum, do not change much varying hole doping in the interval $0.8333 \leq n < 1$. On the other hand, the pairing correlation strength rapidly increases with doping starting from a very small value at half-filling $n = 1$, reaching a maximum around $n \simeq 0.9$, and then further decreasing by hole doping to a negligible value again at $n \sim 0.5$. At the same time, in the $k_{rung} = \pi$ branch of the spectrum, a significant spectral weight redistribution away from the (π, π) wave-vector transfer, characteristic of the half-filled case, is observed as a function of hole-doping. Low energy spin incommensurate features develop. Our results suggest that the vicinity of (π, π) is the portion of the spectrum that is related the most with hole pairing, in agreement with a recent Quantum Monte Carlo study supplemented by Maximum Entropy techniques of the two dimensional Hubbard model [49].

Even though obtained on ladders, our results are consistent with the general picture that emerged from recent RIXS and neutron scattering experiments on two-dimensional cuprates, highlighting again the similarity of the physics of ladders and two-dimensional systems. Indeed, recent RIXS investigations of LSCO [44–46] have found the persistence of high energy magnetic excitations at the antiferromagnetic zone boundary from the underdoped up to the highly overdoped regime where superconductivity disappears. At the same time, neutron scat-

tering experiments have shown that low energy magnetic excitations around the antiferromagnetic zone center are much reduced with doping [47]. In this work we find that, even for ladders, high energy magnetic excitations along the $k_{rung} = 0$ branch do not change much up to large hole dopings, therefore appearing marginal to the pairing mechanism, while the main reason for the reduction of the pairing strength needs to be researched in the spectral weight at low energies around the antiferromagnetic zone center (π, π) .

In order to characterize quantitatively this spectral weight redistribution, we have evaluated the integrated low-energy spin spectral weight around the wave-vector transfer (π, π) as a function of hole doping (see Fig. 9 and Eq. 6). The qualitative similarity of the results shown in Fig. 9 with the pairing strength extracted from a ground state analysis (Fig. 4(b)) suggest that the pairing correlation strength \bar{D}_S could be extracted experimentally directly from the magnetic excitation spectra. A recent neutron scattering study [64] of the spin gap evolution upon doping in the spin-ladder compound $\text{Sr}_{14-x}\text{Ca}_x\text{Cu}_{24}\text{O}_{41}$ has shown progress in the possibility of measuring the full spectrum response of strongly correlated ladders by changing the hole dopings. We urge

neutron scattering experts to carry out inelastic neutron scattering experiments on ladder materials over a wide range of doping to test our theoretical predictions. Because of the clear similarities between cuprate ladders and layers, our conclusions can tentatively be extended to two-dimensional systems as well.

Acknowledgments

The authors acknowledge useful conversations with Prof. C. Batista. A.N. and E.D. were supported by the US Department of Energy (DOE), Office of Basic Energy Sciences (BES), Materials Sciences and Engineering Division. N.P. was supported by the National Science Foundation Grant No. DMR-1404375. The work of G.A. was conducted at the Center for Nanophase Materials Science, sponsored by the Scientific User Facilities Division, BES, DOE, under contract with UT-Battelle. Numerical simulations were performed at the Center for Nanophase Materials Sciences, which is a DOE Office of Science User Facility.

-
- ¹ D. J. Scalapino, Rev. Mod. Phys. **84**, 1383 (2012), URL <https://link.aps.org/doi/10.1103/RevModPhys.84.1383>.
 - ² E. Dagotto, Rev. Mod. Phys. **66**, 763 (1994), URL <https://link.aps.org/doi/10.1103/RevModPhys.66.763>.
 - ³ D. C. Johnston, Advances in Physics **59**, 803 (2010), URL <http://dx.doi.org/10.1080/00018732.2010.513480>.
 - ⁴ A. Chubukov, Annu. Rev. Condens. Matter Phys. **3**, 57 (2012), URL <https://doi.org/10.1146/annurev-conmatphys-020911-125055>.
 - ⁵ P. Dai, J. Hu, and E. Dagotto, Nat. Phys. **8**, 709 (2012), URL <http://dx.doi.org/10.1038/nphys2438>.
 - ⁶ P. Bourges, B. Keimer, S. Pailhès, L. Regnault, Y. Sidis, and C. Ulrich, Physica C: Superconductivity **424**, 45 (2005), URL <http://www.sciencedirect.com/science/article/pii/S0921453405001772>.
 - ⁷ A. Christianson, E. Goremychkin, R. Osborn, S. Rosenkranz, M. Lumsden, C. Malliakas, I. Todorov, H. Claus, D. Chung, M. G. Kanatzidis, et al., Nature **456**, 930 (2008), URL <http://dx.doi.org/10.1038/nature07625>.
 - ⁸ M. D. Lumsden, A. D. Christianson, D. Parshall, M. B. Stone, S. E. Nagler, G. J. MacDougall, H. A. Mook, K. Lokshin, T. Egami, D. L. Abernathy, et al., Phys. Rev. Lett. **102**, 107005 (2009), URL <https://link.aps.org/doi/10.1103/PhysRevLett.102.107005>.
 - ⁹ Y. Qiu, W. Bao, Y. Zhao, C. Broholm, V. Stanev, Z. Tesanovic, Y. C. Gasparovic, S. Chang, J. Hu, B. Qian, et al., Phys. Rev. Lett. **103**, 067008 (2009), URL <https://link.aps.org/doi/10.1103/PhysRevLett.103.067008>.
 - ¹⁰ V. Emery, S. Kivelson, and J. Tranquada, Proceedings of the National Academy of Sciences **96**, 8814 (1999).
 - ¹¹ J. Tranquada, H. Woo, T. Perring, H. Goka, G. Gu, G. Xu, M. Fujita, and K. Yamada, Nature **429**, 534 (2004), URL <http://dx.doi.org/10.1038/nature02574>.
 - ¹² V. Hinkov, S. Pailhès, P. Bourges, Y. Sidis, A. Ivanov, A. Kulakov, C. Lin, D. Chen, C. Bernhard, and B. Keimer, Nature **430**, 650 (2004), URL <http://dx.doi.org/10.1038/nature02774>.
 - ¹³ S. Hayden, H. Mook, P. Dai, T. Perring, and F. Doğan, Nature **429**, 531 (2004), URL <http://dx.doi.org/10.1038/nature02576>.
 - ¹⁴ C. Stock, W. J. L. Buyers, R. A. Cowley, P. S. Clegg, R. Coldea, C. D. Frost, R. Liang, D. Peets, D. Bonn, W. N. Hardy, et al., Phys. Rev. B **71**, 024522 (2005), URL <https://link.aps.org/doi/10.1103/PhysRevB.71.024522>.
 - ¹⁵ S. Pailhès, Y. Sidis, P. Bourges, V. Hinkov, A. Ivanov, C. Ulrich, L. P. Regnault, and B. Keimer, Phys. Rev. Lett. **93**, 167001 (2004), URL <https://link.aps.org/doi/10.1103/PhysRevLett.93.167001>.
 - ¹⁶ J. Tranquada, H. Woo, T. Perring, H. Goka, G. Gu, G. Xu, M. Fujita, and K. Yamada, Journal of Physics and Chemistry of Solids **67**, 511 (2006).
 - ¹⁷ T. A. Maier, S. Graser, D. J. Scalapino, and P. Hirschfeld, Phys. Rev. B **79**, 134520 (2009), URL <https://link.aps.org/doi/10.1103/PhysRevB.79.134520>.
 - ¹⁸ P. Dai, Rev. Mod. Phys. **87**, 855 (2015), URL <https://link.aps.org/doi/10.1103/RevModPhys.87.855>.
 - ¹⁹ D. N. Argyriou, A. Hiess, A. Akbari, I. Eremin, M. M. Korshunov, J. Hu, B. Qian, Z. Mao, Y. Qiu, C. Broholm, et al., Phys. Rev. B **81**, 220503 (2010), URL <https://link.aps.org/doi/10.1103/PhysRevB.81.220503>.
 - ²⁰ D. Liu, W. Zhang, D. Mou, J. He, Y.-B. Ou, Q.-Y. Wang, Z. Li, L. Wang, L. Zhao, S. He, et al., Nat. Commun. **3**, 931 (2012), URL <http://dx.doi.org/10.1038/ncomms1946>.
 - ²¹ S. R. White, Phys. Rev. Lett. **69**, 2863 (1992), URL <https://link.aps.org/doi/10.1103/PhysRevLett.69.2863>.

- //link.aps.org/doi/10.1103/PhysRevLett.69.2863.
- 22 E. Dagotto and T. M. Rice, *Science* **271**, 618 (1996), URL <http://science.sciencemag.org/content/271/5249/618>.
 - 23 E. Dagotto, *Reports on Progress in Physics* **62**, 1525 (1999), URL <http://stacks.iop.org/0034-4885/62/i=11/a=202>.
 - 24 M. Uehara, T. Nagata, J. Akimitsu, H. Takahashi, N. Mori, and K. Kinoshita, *Journal of the Physical Society of Japan* **65**, 2764 (1996), URL <http://dx.doi.org/10.1143/JPSJ.65.2764>.
 - 25 E. Dagotto, J. Riera, and D. Scalapino, *Phys. Rev. B* **45**, 5744 (1992), URL <https://link.aps.org/doi/10.1103/PhysRevB.45.5744>.
 - 26 H. Tsunetsugu, M. Troyer, and T. M. Rice, *Phys. Rev. B* **49**, 16078 (1994), URL <https://link.aps.org/doi/10.1103/PhysRevB.49.16078>.
 - 27 T. A. Maier, D. Poilblanc, and D. J. Scalapino, *Phys. Rev. Lett.* **100**, 237001 (2008), URL <https://link.aps.org/doi/10.1103/PhysRevLett.100.237001>.
 - 28 D. Poilblanc, D. J. Scalapino, and S. Capponi, *Phys. Rev. Lett.* **91**, 137203 (2003), URL <https://link.aps.org/doi/10.1103/PhysRevLett.91.137203>.
 - 29 C. A. Hayward, D. Poilblanc, R. M. Noack, D. J. Scalapino, and W. Hanke, *Phys. Rev. Lett.* **75**, 926 (1995), URL <https://link.aps.org/doi/10.1103/PhysRevLett.75.926>.
 - 30 M. Dolfi, B. Bauer, S. Keller, and M. Troyer, *Phys. Rev. B* **92**, 195139 (2015), URL <https://link.aps.org/doi/10.1103/PhysRevB.92.195139>.
 - 31 D. Poilblanc, E. Orignac, S. R. White, and S. Capponi, *Phys. Rev. B* **69**, 220406 (2004), URL <https://link.aps.org/doi/10.1103/PhysRevB.69.220406>.
 - 32 M. Matsuda, K. Katsumata, R. S. Eccleston, S. Brehmer, and H.-J. Mikeska, *Phys. Rev. B* **62**, 8903 (2000), URL <https://link.aps.org/doi/10.1103/PhysRevB.62.8903>.
 - 33 T. S. Nunner, P. Brune, T. Kopp, M. Windt, and M. Grüninger, *Phys. Rev. B* **66**, 180404 (2002), URL <https://link.aps.org/doi/10.1103/PhysRevB.66.180404>.
 - 34 R. Coldea, S. M. Hayden, G. Aeppli, T. G. Perring, C. D. Frost, T. E. Mason, S.-W. Cheong, and Z. Fisk, *Phys. Rev. Lett.* **86**, 5377 (2001), URL <https://link.aps.org/doi/10.1103/PhysRevLett.86.5377>.
 - 35 G. Roux, S. R. White, S. Capponi, A. Läuchli, and D. Poilblanc, *Phys. Rev. B* **72**, 014523 (2005), URL <https://link.aps.org/doi/10.1103/PhysRevB.72.014523>.
 - 36 F. H. L. Essler and R. M. Konik, *Phys. Rev. B* **75**, 144403 (2007), URL <https://link.aps.org/doi/10.1103/PhysRevB.75.144403>.
 - 37 S. Daul, D. J. Scalapino, and S. R. White, *Phys. Rev. Lett.* **84**, 4188 (2000), URL <https://link.aps.org/doi/10.1103/PhysRevLett.84.4188>.
 - 38 S. Basu, R. J. Gooding, and P. W. Leung, *Phys. Rev. B* **63**, 100506 (2001), URL <https://link.aps.org/doi/10.1103/PhysRevB.63.100506>.
 - 39 F. C. Zhang, *Phys. Rev. Lett.* **90**, 207002 (2003), URL <https://link.aps.org/doi/10.1103/PhysRevLett.90.207002>.
 - 40 T. Xiang, H. G. Luo, D. H. Lu, K. M. Shen, and Z. X. Shen, *Phys. Rev. B* **79**, 014524 (2009), URL <https://link.aps.org/doi/10.1103/PhysRevB.79.014524>.
 - 41 L. Arrachea and D. Zanchi, *Phys. Rev. B* **71**, 064519 (2005), URL <https://link.aps.org/doi/10.1103/PhysRevB.71.064519>.
 - 42 M. Abram, J. Kaczmarczyk, J. Jedrak, and J. Spalek, *Phys. Rev. B* **88**, 094502 (2013), URL <https://link.aps.org/doi/10.1103/PhysRevB.88.094502>.
 - 43 L. J. P. Ament, M. van Veenendaal, T. P. Devereaux, J. P. Hill, and J. van den Brink, *Rev. Mod. Phys.* **83**, 705 (2011), URL <https://link.aps.org/doi/10.1103/RevModPhys.83.705>.
 - 44 M. Dean, R. Springell, C. Monney, K. Zhou, J. Pereiro, I. Božović, B. Dalla Piazza, H. Rønnow, E. Morenzoni, J. Van Den Brink, et al., *Nature Mater.* **11**, 850 (2012), URL <http://dx.doi.org/10.1038/nmat3409>.
 - 45 M. Dean, G. Dellea, R. Springell, F. Yakhou-Harris, K. Kummer, N. Brookes, X. Liu, Y. Sun, J. Strle, T. Schmitt, et al., *Nature Mater.* **12**, 1019 (2013), URL <http://dx.doi.org/10.1038/nmat3723>.
 - 46 S. Wakimoto, K. Ishii, H. Kimura, M. Fujita, G. Dellea, K. Kummer, L. Braicovich, G. Ghiringhelli, L. M. Debeer-Schmitt, and G. E. Granroth, *Phys. Rev. B* **91**, 184513 (2015), URL <https://link.aps.org/doi/10.1103/PhysRevB.91.184513>.
 - 47 S. Wakimoto, K. Yamada, J. M. Tranquada, C. D. Frost, R. J. Birgeneau, and H. Zhang, *Phys. Rev. Lett.* **98**, 247003 (2007), URL <https://link.aps.org/doi/10.1103/PhysRevLett.98.247003>.
 - 48 C. Jia, E. Nowadnick, K. Wohlfeld, Y. Kung, C.-C. Chen, S. Johnston, T. Tohyama, B. Moritz, and T. Devereaux, *Nat. Commun.* **5** (2014), URL <http://dx.doi.org/10.1038/ncomms4314>.
 - 49 E. W. Huang, D. J. Scalapino, T. A. Maier, B. Moritz, and T. P. Devereaux, arXiv preprint arXiv:1705.03949 (2017).
 - 50 D. Meyers, H. Miao, A. C. Walters, V. Bisogni, R. S. Springell, M. d'Astuto, M. Dantz, J. Pelliciari, H. Y. Huang, J. Okamoto, et al., *Phys. Rev. B* **95**, 075139 (2017), URL <https://link.aps.org/doi/10.1103/PhysRevB.95.075139>.
 - 51 K. A. Chao, J. Spalek, and A. M. Oles, *Journal of Physics C: Solid State Physics* **10**, L271 (1977), URL <http://stacks.iop.org/0022-3719/10/i=10/a=002>.
 - 52 R. M. Noack, S. R. White, and D. J. Scalapino, *EPL (Europhysics Letters)* **30**, 163 (1995), URL <http://stacks.iop.org/0295-5075/30/i=3/a=007>.
 - 53 R. Noack, S. White, and D. Scalapino, *Physica C: Superconductivity* **270**, 281 (1996), ISSN 0921-4534, URL <http://www.sciencedirect.com/science/article/pii/S0921453496005151>.
 - 54 H. Endres, R. M. Noack, W. Hanke, D. Poilblanc, and D. J. Scalapino, *Phys. Rev. B* **53**, 5530 (1996), URL <https://link.aps.org/doi/10.1103/PhysRevB.53.5530>.
 - 55 E. Jeckelmann, D. J. Scalapino, and S. R. White, *Phys. Rev. B* **58**, 9492 (1998), URL <https://link.aps.org/doi/10.1103/PhysRevB.58.9492>.
 - 56 R. M. Noack, N. Bulut, D. J. Scalapino, and M. G. Zacher, *Phys. Rev. B* **56**, 7162 (1997), URL <https://link.aps.org/doi/10.1103/PhysRevB.56.7162>.
 - 57 S. R. White, I. Affleck, and D. J. Scalapino, *Phys. Rev. B* **65**, 165122 (2002), URL <https://link.aps.org/doi/10.1103/PhysRevB.65.165122>.
 - 58 J. Riera, D. Poilblanc, and E. Dagotto, *The European Physical Journal B - Condensed Matter and Complex Systems* **7**, 53 (1999), ISSN 1434-6036, URL <http://dx.doi.org/10.1007/s100510050588>.
 - 59 D. J. Scalapino and S. R. White, *Phys. Rev. B* **58**, 8222 (1998), URL <http://link.aps.org/doi/10.1103/>

- PhysRevB.58.8222.
- ⁶⁰ T. D. Kühner and S. R. White, Phys. Rev. B **60**, 335 (1999), URL <http://link.aps.org/doi/10.1103/PhysRevB.60.335>.
- ⁶¹ A. Nocera and G. Alvarez, Phys. Rev. E **94**, 053308 (2016), URL <https://link.aps.org/doi/10.1103/PhysRevE.94.053308>.
- ⁶² A. Nocera, N. D. Patel, J. Fernandez-Baca, E. Dagotto, and G. Alvarez, Phys. Rev. B **94**, 205145 (2016), URL <https://link.aps.org/doi/10.1103/PhysRevB.94.205145>.
- ⁶³ See Supplemental Material at [URL will be inserted by publisher] for a description and usage of the computer code.
- ⁶⁴ G. Deng, N. Tsyrlin, P. Bourges, D. Lamago, H. Ronnow, M. Kenzelmann, S. Danilkin, E. Pomjakushina, and K. Conder, Phys. Rev. B **88**, 014504 (2013), URL <https://link.aps.org/doi/10.1103/PhysRevB.88.014504>.